

4. Methodology

Sediment sources can be complex and difficult to accurately recognize. Studies identifying these sources utilize a multitude of field, laboratory, and computer modeling techniques. Traditional methods include aerial photograph analysis supported by field observations and data collection (Collins *et al.* 2001; WFPB 1997a) and implementation of profilometers and erosion pins (Hooke 1979; Couper and Maddock 2001; Prosser *et al.* 2000). More technical studies frequently employ quantitative analyses incorporated into a Geographic Information System (GIS) model (DeRose *et al.* 1998; Millward and Mersey 1999; Dai and Lee 2001; Parsons and Abrahams 1993; Finco and Hepner 1998) or analyzed in conjunction with aerial photography and field data (Aniya 1985). More complex technologies have enabled the origin and dating of sediments based on floodplain cores by analyzing element content relative to source composition (Magilligan 1985; Pasternack *et al.* 2001; Owens and Walling 2002) and “fingerprinting” derived from sediment size and composition to identify sources (Clapp *et al.* 2002; Collins and Walling 2002).

Using aerial photographs, field data collection, and information from local land managers, sediment sources can be identified (WFPB 1997a). The methods used in this study incorporated these techniques and supplemented them with qualitative values derived from GIS modeling. Through these methods, sediment production from mass wasting, surface erosion, and some fluvial erosion processes were identified and assessed. While these are naturally occurring processes, urbanization in the form of development, roads, and trails, which is prevalent throughout the watershed, exacerbates sediment production enhancing the amount of sediment that is delivered to a drainage network. Natural and anthropogenic sources were distinguished by “triggers” and amounts of material delivered to the stream network quantified where possible.

Aerial photographic interpretation, GIS analyses, and field data collection were the main methods used to identify sediment sources throughout the upper watershed. Landslides and large gullies were observed from an aerial photographic survey and digitized into a GIS. Field survey data used in conjunction with GIS identified additional site-specific source areas. Volume of erosion was calculated where the general erosion was severe and localized enough to make an accurate estimate. A complete quantitative assessment of surface erosion processes including soil creep, sheetwash, and rainsplash erosion could not be quantitatively considered without a long-term monitoring study employing techniques, such as erosion pins.

The findings for this study were collected and analyzed in multiple steps. A trail and road assessment was conducted with the simultaneous collection, modification, and modeling of GIS data, including the Soil Erodibility Model (SEM), perennial flow points, effective drainage density, connectivity, and land use change. Select landslides and gullies were subsequently mapped in the field and from stereo aerial photographs. A shallow slope stability model, SHALSTAB, was used to estimate relative landslide susceptibility throughout the watershed. Finally, source areas were identified with the synthesis of findings, and prioritizations for management were made.

4.1 Aerial Photographic Interpretation

Aerial photographic interpretation provides valuable and accurate assessments of geomorphic and land use changes. It is a commonly used technique to assess mass wasting using a visual history of change. By evaluating sequential historical photographs, large areas with barren soil, mainly gullies, and those where past and recent mass wasting events have occurred can be readily identified and can be related to land use changes over time, such as urban development, farming, and ranching.

The U.S. Geological Survey (USGS) has created and compiled a wealth of data on landslides in San Mateo County, California using aerial photographic interpretation. Maps were originally created to evaluate geology, existing landslide deposits, and slope (Nilsen 1986). These findings were then analyzed to create a relative slope-stability map (Figure 35) (Brabb *et al.* 1972) that has since been updated and is now available in GIS format (Ellen *et al.* 1997). While these maps provide a foundation for determining landslide potential, and hence sediment sources, on a regional scale, a significantly more detailed map was generated in a portion of the South and Sanchez subwatersheds in SPCW as a result of numerous slides throughout the San Francisco Bay area, including 475 in the greater Pacifica area alone, during the January 1982 storm event (Figures 36a, b, and c) (Smith 1988). The previous landslide maps mainly identify large, deep-seated slides until the storm revealed the prevalence and potential of smaller, shallow slides (Ellen *et al.* 1988). The storm prompted extensive research on these smaller, fast moving debris flows predominantly using aerial photographs throughout the SF Bay region.

Washington State Department of Natural Resources Forest Practice Board (WFPB) has developed a commonly utilized method to categorize areas for landslide potential (Dietrich *et al.* 1998). This method uses aerial photography to conduct an inventory of disturbed areas followed by field inspections to validate these findings. These results are then extrapolated to areas with similar characteristics including geology and topography. The likelihood of future mass wasting events can then be spatially predicted based on these results (WFPB 1997a).

A method similar to that developed by the WFPB was used for an extensive study conducted on a San Francisco Bay area watershed, Wildcat Creek. This method utilized stereo aerial photographs to identify active and inactive landslides as well as the headward extension of tributaries (Collins *et al.* 2001). Coupled with field assessment, sediment input from these slides was estimated and field observations identified additional slides in heavily vegetated areas not visible in aerial photographs.

Methods similar to those developed by WFPB were employed to identify mass wasting and select surface erosion occurrences in SPCW in this study. Through aerial photographic interpretation landslides were identified and the scar area, track, date of occurrence, and possible triggers of mass wasting events in SPCW was revealed. The volume of debris flows was calculated based on the surface area obtained from the aerial photographs times the average depth between the deepest and shallowest depths of large landslides occurring in the

area. The average of these landslide depths was generated from a literature review. The total volume displaced from mass wasting events was

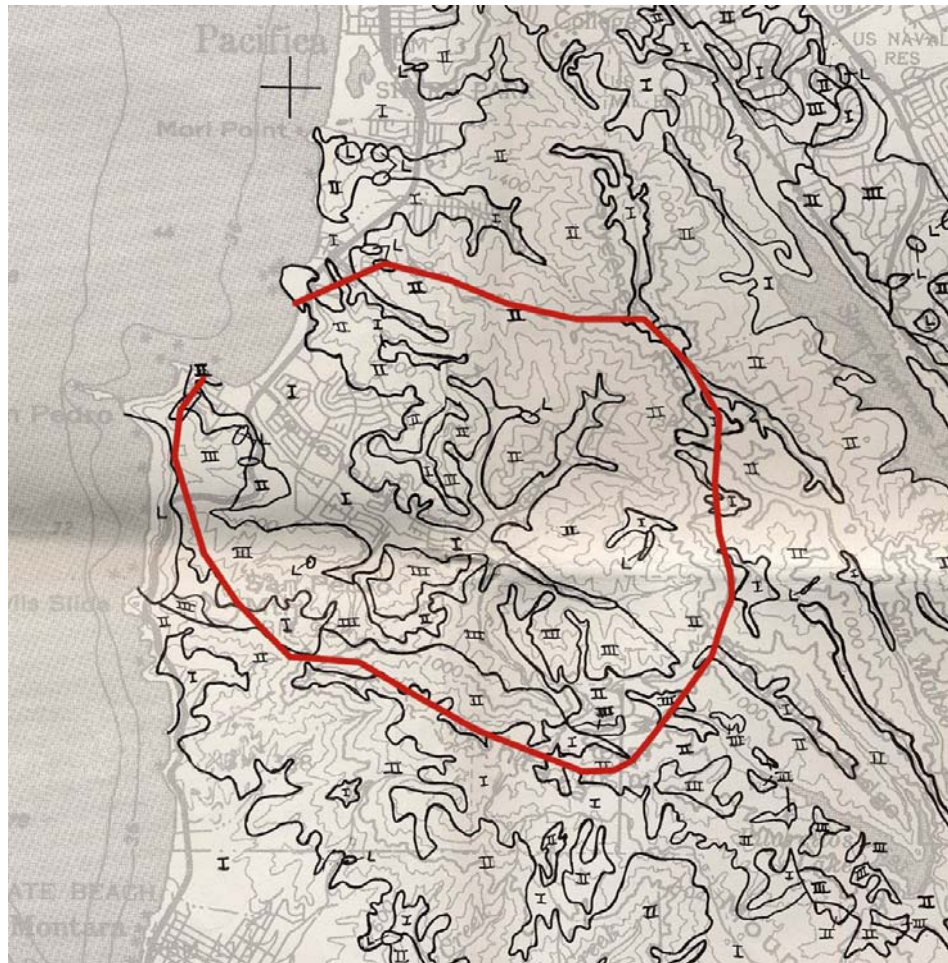


Figure 35: Generalized relative slope susceptibility map of SPCW (shown in red) at 1:62,500. Ranges on a scale of most stable at I to least stable at III (Brabb *et al.* 1972).



Figure 36a: Pre-1982 debris flow scars and tracks mapped from aerial photographs. Originally mapped at 12K, large portions of the Sanchez, South, and Middle Subwatersheds are covered (Smith 1988).

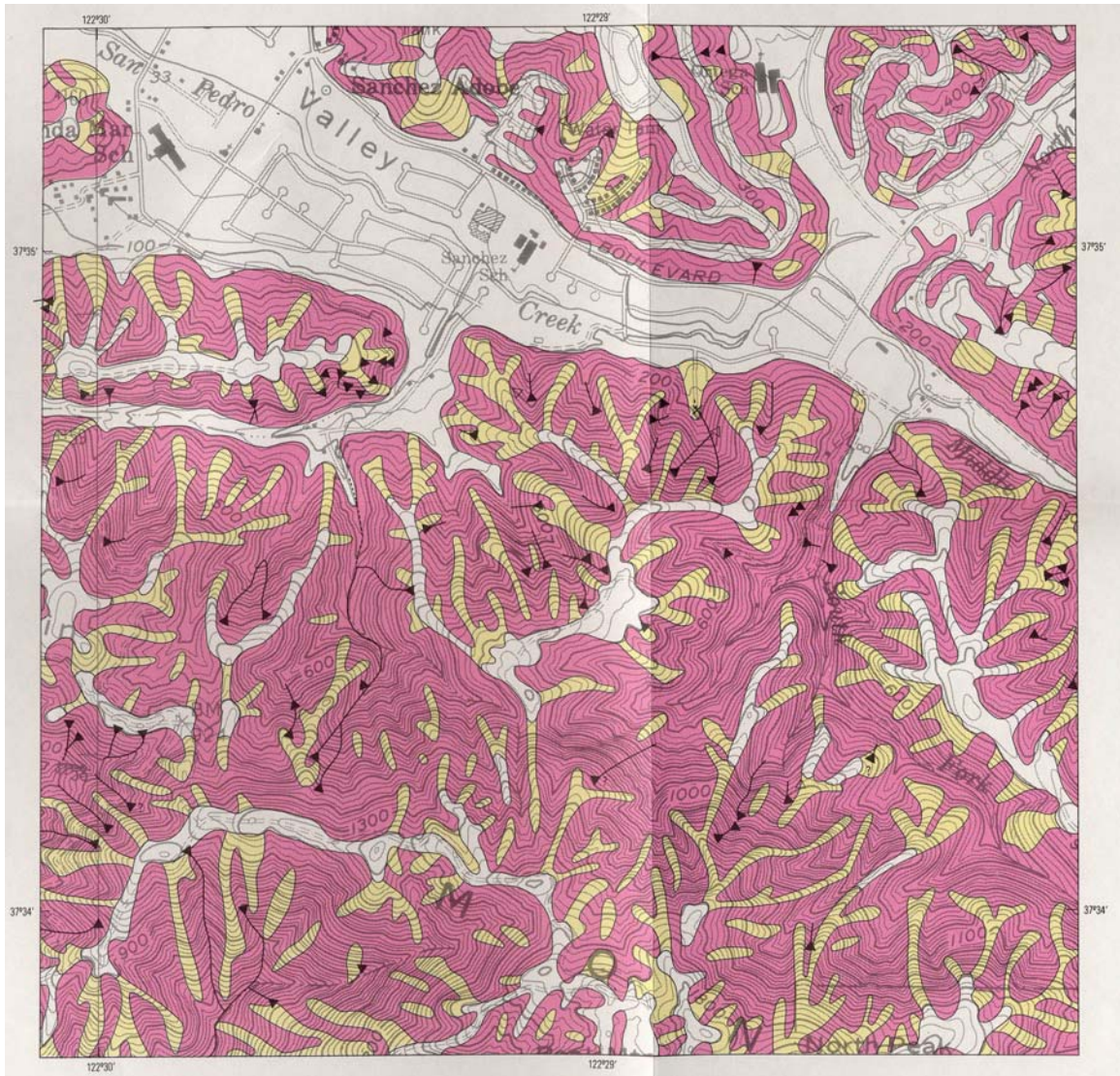


Figure 36b: Landslides and tracks from the 1982 storm event superimposed on a 1977 susceptibility map previously created by the author. The pink areas are the most susceptible, the yellow are intermediate, and white are the least (Smith 1988).



Figure 36c: Debris flow susceptibility map updated from the 1977 version with likely debris flow runout paths (Smith 1988).

calculated and the amount delivered was based on the proximity of deposition to the stream network. Gullies were also mapped from the aerial photographs but volume estimates were not estimated.

The number of landslides identified using the aerial photographic interpretation techniques depends mainly on the year the photography was taken relative to the occurrence of a landslide (Dietrich *et al.* 1998). For this reason, photographs from six different years with reference to corresponding ancillary data were analyzed: 1941 at a scale of 1:24,000, 1955 at 1:10,000, and 1975, 1983, 1991, and 1997 at 1:12,000. Gullies, landslide scarps, and obvious landslide tracks digitized into ArcMap 8.2 where they were analyzed in conjunction with existing layers, such as slope, geology, and soil. Land uses and trails were also digitized into a GIS from each of these years while landslides and gullies were mapped from all but 1991. The land uses were divided into three groups: developed, farmland/rangeland, and other, which includes natural and as of yet undeveloped lands. Approximate dates of land conversion, based on the year of the photograph where a change was observed, were also documented with the progression of development. Trails were attributed with dates of construction, levels of use, and levels of maintenance, and roads were coded with dates of construction. A few of the pre-existing trails that have since overgrown and been decommissioned were not included on the maps. Ancillary photographs at various scales supplemented the stereo photos with additional information including dates of trail and road construction, but were not directly mapped (see Appendix A for a complete list of photographs used).

4.2 Field Surveys

In sediment source analysis studies, field surveys are still the predominant method to accurately identify localized areas contributing to water quality deterioration and associated watershed degradation. They are particularly useful for total maximum daily load studies to determine sediment yield and sometimes the entire sediment budget of a watershed (Stillwater Sciences 1999; PWA 2003).

Field surveys of hillslopes help verify the findings of aerial photographic interpretation and GIS models. Detailed surveys identify specific areas of sediment delivery to the drainage network mainly from anthropogenic sources as these trails and roads provide access to the watersheds. Surveying these anthropogenic areas in great detail biases the results, as the natural sources are more difficult to access and can't be as readily identified in the field.

Site-specific land use impacts are revealed through field surveys. Direct correlations between mass wasting events and the physical trigger mechanisms that caused the incidents, including concentrated flow from a culvert or drainage ditch, are readily identified (WFPB 1997b; Bullard *et al.* 2002). These features are apparent on a small scale and can often be attributed to the spatial proximity of the associated trigger mechanism.

Findings from the aerial photographs and GIS analyses were considered in the field while evaluating local geomorphic variations. Volume from several sizeable and readily accessible gullies was estimated from cross-sectional area and depth. Anthropogenic sources triggering

surface erosion and landslides were identified and volumes of smaller sources visually estimated through a trail and road assessment. Most of the trails and some of the roads likely to be producing sediment with connectivity to the stream network were surveyed.

4.3 GIS Models

A GIS provides a valuable method of displaying and analyzing spatial data. Correlations between the multiple factors involved in sediment production can be investigated. These models make predictions based on underlying variables and visually display spatial relationships that would otherwise not be seen. Equations such as the Universal Soil Loss Equation (USLE) are often inputs for empirical models with each factor of the equation acting as a layer that spatially represents a known value. The USLE can be used to derive a layer of predicted soil loss based on inputs, such as sediment yield measurements. Deterministic models, such as the Shallow Slope Stability Model (SHALSTAB) are often based on known physical processes or relationships but require data on all contributing inputs. As a result, these models can only be applied to landscapes for which all contributing geomorphic processes are well represented by the model.

4.3.1 SHALSTAB

Landslide susceptibility models have been created mostly for safety reasons as they present a significant hazard to human inhabitants of steep-sloped hill and mountain areas. Since shallow landslides are an important source of sediment (Dietrich *et al.* 1998) and are often a direct result of land use, these models also apply to sediment source analysis studies. The Shallow Slope Stability Model (SHALSTAB) is one such deterministic model that the potential of shallow landslides across a study site, which frequently result in debris flows (Dietrich *et al.* 1998).

SHALSTAB is a deterministic GIS model based on research conducted by Montgomery and Dietrich used to analyze relative shallow landslide potential (Dietrich *et al.* 1998). Building on methods developed by the WFPB, this model shifts away from establishing geomorphologically similar mass wasting units to analyze areas of instability. This operator-interpreted method introduces a larger element of human error that SHALSTAB is able to minimize. Initial aerial photographic assessment integrated with field data collection generates a detailed landslide inventory, which can then be used to test the results of SHALSTAB. Analyzed with a digital elevation model data the relative slide susceptibility throughout the entire SPCW is determined and tested against known landslides.

SHALSTAB is a parameter free model that runs on the foundation of process driven elements of fluvial-induced geomorphic change. The model is based on the understanding of how fluvial processes interact with soil and underlying bedrock to generate landslides. Extensive field studies have been conducted in Oregon and multiple locations in northern California to modify and validate the results (Dietrich *et al.* 1998). Using digital elevation model data, the relative slope stability of a landscape is determined at which landslides may occur under steady state rainfall conditions (Dietrich and Montgomery 1998).

Slope stability and hydrologic flow models compose the foundation of SHALSTAB (Dietrich and Montgomery 1998). Slope stability is calculated using an infinite slope form of the Mohr-Coulomb equation as a function of the strength of resistance from cohesion and the frictional resistance on the failure plane. This equation was modified to remove the cohesion factor because of the difficulty in gathering such data as a result of the variability of its influence across multiple landscapes. Instead the friction angle was set to 45° to compensate for lack of root cohesion consideration. The modified equation

$$\frac{h}{z} = \frac{\rho_s}{\rho_w} \left(1 - \frac{\tan \nu}{\tan \phi} \right) \quad (1)$$

calculates the proportion of the soil column that is saturated at the point of instability, h/z , where h is the water level above the failure plane (m), z is the soil depth (m), ρ_s is the soil bulk density (1,200 kg m⁻³), ρ_w is the water density (1,000 kg m⁻³), ν is the slope angle (°), and ϕ is the angle of internal friction in the soil (45°) (Dietrich *et al.* 1998). The model was initially run with the soil bulk density of 1,700 kg m⁻³ with disappointing results. Subsequent iterations were conducted with the soil bulk density of 1,010 kg m⁻³, 1,200 kg m⁻³, and 1,500 kg m⁻³. As the soil bulk density for the study area and the various soil types is unknown, the model run with the value of 1,200 kg m⁻³ was analyzed with the best results.

The hydrologic flow model calculates steady-state subsurface flow based on soil transmissivity, the ability of subsurface flow to transmit water downslope, and Darcy's Law (Dietrich and Montgomery 1998), which determines the flow-through rate as a function of hydraulic conductivity, hydraulic gradient, and the cross-sectional area through which the subsurface water flows (Ahnert 1996). In the modified hydrologic flow model runoff is understood to be generated by shallow subsurface flow and saturation overland flow:

$$\frac{h}{z} = \frac{q}{T} \frac{a}{b \sin \nu} \quad (2)$$

q is the effective rainfall (rainfall minus evapotranspiration in mm/day), T is the soil transmissivity (m²/day), b is the hillslope width (m), a is the subsurface flow drainage area (m²), and ν is the degrees slope (Dietrich *et al.* 1998). The variables a , b , and ν were calculated from contributing area and slope grids generated as one of the steps in the model. Finally, both the slope stability and the hydrologic flow models are integrated in SHALSTAB to predict the magnitude of relative slope stability:

$$\frac{q}{T} = \frac{\rho_s}{\rho_w} \left(1 - \frac{\tan \nu}{\tan \phi} \right) \frac{b}{a} \sin \nu \quad (3)$$

This combined equation is expressed as the hydrologic ratio of the effective rainfall to soil transmissivity, which designates slope stability (Dietrich and Montgomery 1998).

The final product indicating shallow slope stability, q/T is best displayed in logarithmic form as the results range over multiple orders of magnitude (Dietrich *et al.* 1998). The slope stability value is expressed in negative values and the lower the value, the more unstable the slope. Slopes are chronically unstable below -3.1 as it is not likely that a rainfall event of the intensity needed to cause slopes to fail with this ranking will occur in nature. The results can also be displayed in ordinal classification as threshold values created by Dietrich and Montgomery ranging from low to high slope instability, or chronically stable to chronically unstable (Dietrich and Montgomery 1998). Anthropogenic influences such as roads and trails were not considered in the model were analyzed with the final results to identify more localized areas of potential instability.

Creating a SHALSTAB model for SPCW followed the general outline proposed by Dietrich and Montgomery (1998). The only initial data needs were digital elevation model from which various layers were derived and landslide data which was used to validate the accuracy of the calculated q/T values. As the available digital elevation model is based on the most recent hillslope topography, landslides that occurred in areas that have since been at least partially leveled and subsequently developed were removed from consideration in the model. SHALSTAB can be run with digital elevation data alone but within the constraints of this model were tested against the known landslide distribution. The model was very applicable to SPCW as it has similar topographic and geologic characteristics for which SHALSTAB has previously been modified and tested. In addition, the visible landslides were mapped and provided a good test against which to analyze the results.

4.3.2 Soil Erodibility Model

While not as significant as landslides in generating sediment, surface erosion does occur in SPCW. A simple soil erodibility model, the SEM, incorporates empirical data from % slope and a physical soil property, the K-factor, to generate a rating system (WFPB 1997b). As land uses significantly enhance and deliver surface erosion to the drainage network, this model can be readily compared to urbanization practices in SPCW. In contrast, vegetation acts as a buffer abating sediment delivery to the drainage network and was incorporated to the surface erosion analysis.

The most commonly used soil erodibility model is the Universal Soil Loss Equation (USLE), which is integrated into a GIS to calculate empirical data to derive long-term average soil losses (Battad 1993). Best used for predicting surface erosion primarily in agricultural lands (Ahnert 1996), the utility of the equation on forests

and rangelands is questionable (Battad 1993). While the model is not generally applicable to areas influenced by mass wasting, the dominant process in SPCW, Equation 4 presents the interrelatedness of the variables influencing soil erosion (Selby 1993).

The USLE has since been modified to the Revised Universal Soil Loss Equation (RUSLE), which maintains the original values, but incorporates more parameters to improve the effectiveness of the model (Battad 1993). The average annual soil loss, A ($t\ ha^{-1}\ yr^{-1}$), is calculated with the equation:

$$A = LS * R * K * C * P \quad (4)$$

where LS = combined slope steepness and slope length measurements (unitless), R = the rainfall erosivity factor ($\text{MJ mm ha}^{-1} \text{h}^{-1} \text{yr}^{-1}$), K = soil erodibility factor or the soil loss per rainfall erosion index unit as measured on a unit plot ($\text{t ha h MJ}^{-1} \text{mm}^{-1} \text{ha}^{-1}$), C = land cover and management factor, including land use and surface cover and roughness, which estimates the soil loss ratio (unitless), and P = the soil loss ratio of specific support practice factors including terracing and contouring (unitless) (Millward and Mersey 1999; Battad 1993; Marsh 1998; Simanton and Renard 1993). With these modifications RUSLE is able to be adapted to watersheds with varying geomorphology. For example, Millward and Mersey (1999) successfully applied RUSLE to a watershed after further modification of the LS variable to account for steep relief within their study area.

A very basic equation derived from RUSLE, the soil erodibility model (SEM), considers only the K -factor and slope values, or $A = K * S$, where K = the K -factor designated by the Soil Conservation Service (unitless) (Kashiwagi and Hokholt 1991) and S = % slope (WFPB 1997b). This model was modified slightly to better represent the range of k -factor values occurring in SPCW. The model output is classified into a range of low to high erodibility ratings (Table 1). This rating overlaid with land uses identifies anthropogenic sources of sediment. As surface erosion is secondary in the effectiveness of generating sediment to mass wasting within SPCW, it is not expected to be significant except where heavily affected by land use practices. Urbanization in the form of roads, trails, and development on the fringe of hillslopes are the predominant and most influential land use variables in terms of surface erosion production and sediment delivery to the drainage network. This model provided a simple, yet effective measure against which these land uses were then field surveyed to determine the most significant, localized sediment sources produced from surface erosion.

Slope Class (Percent)	$K < 0.25$ Not easily detached	$0.25 < K < 0.40$ Moderately detachable	$K > 0.40$ Easily detached
< 30	Low	Low	Moderate
30 – 65	Low	Moderate	High
> 65	Moderate	High	High

Table 1: Modified soil erodibility ratings derived from the K - factor and slope (WFPB 1997b).

4.3.3 Other GIS

Other GIS models and raster layers generated include the level of connectivity, effective drainage density, and perennial flow initiation. Connectivity, the likelihood of sediment delivery to the stream network, was used to determine the volume of sediment delivered to the tributaries from landslides and gullies. Delivery of sediment from potential sources to the drainage network was considered in all steps of the assessment. Because not all sediment from landslides becomes entrained in the streams (WFPB 1997a), recognizing the connectivity of sources to the drainage network is imperative when analyzing input. While this is also true for surface erosion, only surface erosion in relatively close proximity to the drainage network was considered. Estimates of connectivity compared with the SEM and

SHALSTAB models also revealed contributing areas susceptible to surface erosion and unstable slopes. The total sum of the lengths of drainages including roads, trails, hillslope drainage channels, and tributaries were compiled per subwatershed to determine the effective drainage density. Known pour points along the tributaries where surface perennial flow initiates were also modeled into a layer revealing drainage surface area required to maintain year-round flow. These models are examined in more detail in the Results section.

GIS is integrated with field data throughout the assessment. Ancillary data layers supplemented and supported the findings derived from the raster GIS models SHALSTAB and the SEM. Digitized landslide data derived from the aerial photography and 10-m DEMs were used to run the ArcView 3.2 extension, SHALSTAB, from which the relative slope stability was extrapolated across the entire study area. These results were compared with roads, trails, and land uses to identify additional areas of potential site-specific sources that are not evaluated within the context of this model. Field mapped landslides and gullies were analyzed in ArcMap 8.2 to calculate the volume of displaced sediment. The SEM was also generated using ArcMap 8.2. Again, current roads, trails, and land uses were compared with the final model to determine areas that were delivering enhanced levels of sediment as a result of anthropogenic influence. In contrast, the presence of vegetation and low gradient slopes were considered to determine areas where connectivity was abated.

Most layers are in both vector and raster format and analyzed in ArcView 3.2, ArcMap 8.2, and ArcInfo 4.0. All GIS layers are projected in UTM zone 10N using North American Datum 1983 and a complete list of those used is available in Appendix B.

4.4 Previous Work in SPCW

Several studies have been conducted in SPCW to assess properties of the channel and surrounding hillslopes. Collins *et al.* (2001) provided invaluable data on past and current main channel conditions and found that many stream channel alterations are explained by patterns of land use change. The USGS has repeatedly mapped geologic

properties, landslides deposits, and hillslope stability within SPCW on regional scales (Brabb and Pampeyan 1972; Brabb *et al.* 1972) and highly localized scales (Smith 1988). These studies have contributed to an improved understanding of processes triggering

debris flows, the types of landslides that are most significant in delivering sediment to the drainage network. In addition, detailed and readily accessible GIS data provided by the SPCWC and federal agencies were utilized throughout.

4.5 Synthesis

Compiling the findings generated a comprehensive analysis of sediment source assessment. Site-specific points of erosion identified from aerial photographic interpretation were integrated into a GIS to determine level of connectivity and if possible quantities of delivery. Sources were classified into erosion types and collectively considered as triggered by either natural or anthropogenic activity. Based on this assimilation and levels of connectivity, predictions about the amount of sediment generated for specific drainage areas were made.

Extremely thick and impenetrable vegetative cover dominates the undeveloped hillslopes and tributaries of SPCW, significantly hampering access to the majority of the watershed. Recent fire suppression practices enhance the vegetation density compounding the problem. Aerial photographs and GIS models provide sediment source information without direct access to the watershed. These methods produced both quantitative and qualitative data, which were supplemented with field data collection from relatively accessible portions of the watershed. Ancillary GIS layers including land use, vegetation, and geology facilitated the overall analysis. Finally, based on these findings, areas were prioritized for implementation of sediment abatement measures and management recommendations proposed for adoption.